Scalable Track Initiation for Optical Space Surveillance

Paul W. Schumacher, Jr., Ph.D.
Technical Lead, HSAI-SSA
Air Force Research Laboratory, Kihei, HI

Matthew P. Wilkins, Ph.D.
Senior Engineer
Schafer Corporation

ABSTRACT

The computational complexity of track initiation, also known as initial orbit determination or IOD, using only angle measurements is polynomial in the number of observations. However, the polynomial degree can be high, always at least cubic and commonly quartic or higher. Therefore, practical implementations require attention to the scalability of the algorithms, when one is dealing with the very large number of observations from large surveillance telescopes. We address two broad categories of algorithms. The first category includes and extends the classical methods of Laplace and Gauss, as well as the more modern method of Gooding, in which one solves explicitly for the apparent range to the target in terms of the given data. We find that the orbit solutions (data association hypotheses) can be ranked by means of a concept we call *persistence*, in which a simple statistical measure of likelihood is based on the frequency of occurrence of combinations of observations in consistent orbit solutions. However, range-solution methods can be expected to perform poorly if the initial orbit solutions of most interest are not well conditioned. The second category of algorithms addresses this difficulty. Instead of solving for range, these methods attach a set of range hypotheses to each measured line of sight. Then all pair-wise combinations of observations are considered and the family of Lambert problems is solved for each pair. These algorithms also have polynomial complexity, though now the complexity is quadratic in the number of observations and also quadratic in the number of range hypotheses. We offer a novel type of admissible-region analysis, constructing partitions of the orbital element space and deriving rigorous upper and lower bounds on the possible values of the range for each partition. This analysis allows us to parallelize with respect to the element partitions and to reduce the number of range hypotheses that have to be considered in each processor simply by making the partitions smaller. We present numerical results based on simulated data sets.

1. MOTIVATION

The advent of high-sensitivity, high-capacity optical sensors for space surveillance presents us with interesting and challenging tracking problems. Accounting for the origin of every detection made by such systems is generally agreed to belong to the "most difficult" category of tracking problems. Especially in the early phases of the tracking scenario, when a catalog of targets is being compiled, or when many new objects appear in space because of on-orbit explosion or collision, one faces a combinatorially large number of orbit (data association) hypotheses to evaluate. The number of hypotheses is reduced to a more feasible number if observations close together in time can, with high confidence, be associated by the sensor into extended tracks on single objects. Most current space surveillance techniques are predicated on the sensor systems' ability to form such tracks reliably. However, the required operational tempo of space surveillance, the very large number of objects in Earth orbit and the difficulties of detecting dim, fast-moving targets at long ranges means that individual sensor track reports are often inadequate for computing initial orbit hypotheses. In fact, this situation can occur with optical sensors even when the probability of detection is high. For example, the arc of orbit that has been observed may be too short or may have been sampled too sparsely to allow well-conditioned, usable orbit estimates from single tracks. In that case, one has no choice but to solve a data association problem involving an unknown number of targets and many widely spaced observations of uncertain origin. In the present paper, we are motivated by this more difficult aspect of the satellite cataloging problem. However, the results of this analysis may find use in a variety of less stressing tracking applications.

One method for track initiation from the asteroid community is the use of admissible regions [1] [2]. This work has been adapted for use in tracking Earth orbiting objects by Dan Scheeres and his group at University Colorado – Boulder [3]. However, this methodology was developed by astronomers who had access to many nights of data for relatively slow moving objects (from an Earth point of view), and it requires simultaneous angle and angle rate data

Report Documentation Page		*Form Approved* *OMB No. 0704-0188*

Public reporting burden for the collection of information is estimated to average 1 hour per response, including the time for reviewing instructions, searching existing data sources, gathering and maintaining the data needed, and completing and reviewing the collection of information. Send comments regarding this burden estimate or any other aspect of this collection of information, including suggestions for reducing this burden, to Washington Headquarters Services, Directorate for Information Operations and Reports, 1215 Jefferson Davis Highway, Suite 1204, Arlington VA 22202-4302. Respondents should be aware that notwithstanding any other provision of law, no person shall be subject to a penalty for failing to comply with a collection of information if it does not display a currently valid OMB control number.

1. REPORT DATE **SEP 2012**	2. REPORT TYPE	3. DATES COVERED **00-00-2012 to 00-00-2012**
4. TITLE AND SUBTITLE **Scalable Track Initiation for Optical Space Surveillance**		5a. CONTRACT NUMBER
		5b. GRANT NUMBER
		5c. PROGRAM ELEMENT NUMBER
6. AUTHOR(S)		5d. PROJECT NUMBER
		5e. TASK NUMBER
		5f. WORK UNIT NUMBER
7. PERFORMING ORGANIZATION NAME(S) AND ADDRESS(ES) **Air Force Research Laboratory,Technical Lead, HSAI-SSA,Kihei,HI**		8. PERFORMING ORGANIZATION REPORT NUMBER
9. SPONSORING/MONITORING AGENCY NAME(S) AND ADDRESS(ES)		10. SPONSOR/MONITOR'S ACRONYM(S)
		11. SPONSOR/MONITOR'S REPORT NUMBER(S)

12. DISTRIBUTION/AVAILABILITY STATEMENT **Approved for public release; distribution unlimited**

13. SUPPLEMENTARY NOTES **In Advanced Maui Optical and Space Surveillance Technologies Conference (AMOS), 11-14 Sep 2012, Maui, HI.**

14. ABSTRACT

The computational complexity of track initiation, also known as initial orbit determination or IOD, using only angle measurements is polynomial in the number of observations. However, the polynomial degree can be high, always at least cubic and commonly quartic or higher. Therefore, practical implementations require attention to the scalability of the algorithms, when one is dealing with the very large number of observations from large surveillance telescopes. We address two broad categories of algorithms. The first category includes and extends the classical methods of Laplace and Gauss, as well as the more modern method of Gooding, in which one solves explicitly for the apparent range to the target in terms of the given data. We find that the orbit solutions (data association hypotheses) can be ranked by means of a concept we call persistence, in which a simple statistical measure of likelihood is based on the frequency of occurrence of combinations of observations in consistent orbit solutions. However, range-solution methods can be expected to perform poorly if the initial orbit solutions of most interest are not well conditioned. The second category of algorithms addresses this difficulty. Instead of solving for range, these methods attach a set of range hypotheses to each measured line of sight. Then all pair-wise combinations of observations are considered and the family of Lambert problems is solved for each pair. These algorithms also have polynomial complexity, though now the complexity is quadratic in the number of observations and also quadratic in the number of range hypotheses. We offer a novel type of admissible-region analysis, constructing partitions of the orbital element space and deriving rigorous upper and lower bounds on the possible values of the range for each partition. This analysis allows us to parallelize with respect to the element partitions and to reduce the number of range hypotheses that have to be considered in each processor simply by making the partitions smaller. We present numerical results based on simulated data sets.

15. SUBJECT TERMS					
16. SECURITY CLASSIFICATION OF:			17. LIMITATION OF ABSTRACT	18. NUMBER OF PAGES	19a. NAME OF RESPONSIBLE PERSON
a. REPORT **unclassified**	b. ABSTRACT **unclassified**	c. THIS PAGE **unclassified**	**Same as Report (SAR)**	**10**	

or the ability to synthesize those data from observed quantities. For GEO objects, we typically have only angles data. Our ability to estimate angle rate is limited. Hence, the usefulness of this method for our purpose is equally limited but nevertheless has shown some promise in analyses by Scheeres' group. Without having angle rate available, we still have the option to use the angles data in conjunction with guesses for range. The range guesses could be given in a predetermined sequence over some allowable set of values or could be sampled randomly. In either case, the allowable set of range values would be bounded by constraints derived from the allowable set of orbital elements used for the track initiation. Then Lambert's Theorem would be used to generate a set of initial orbit hypotheses for each pair of measured lines of sight. Lambert's Theorem states that the time of flight between two positions in space depends only on the semi-major axis of the orbit and the position vectors themselves. Hence, two positions and the time of flight between them completely specify the orbit. Alternatively, we can seek to solve for the range at each observation time by imposing dynamical constraints. This approach has higher computational complexity but yields higher confidence earlier in the orbit determination process. To speed up this process, we seek to reduce the number of hypotheses *a priori*. First, we apply geometrical boundaries on range hypotheses. These boundaries may be somewhat overbroad to ensure that the actual orbit lies within the search space. Second, we solve iteratively for ranges and use the geometrical boundaries to screen out bad solutions.

How should we limit the number of range hypotheses to make the total number of candidate orbits manageable while also generating candidates that are likely to correspond to real orbits of interest? Let us seek to generate hypotheses for orbits that lie only in a bounded region of semimajor axis a, eccentricity e, inclination I and right ascension of the ascending node Ω, namely, within a partition specified by the intervals $[a_{MIN}, a_{MAX}]$, $[e_{MIN}, e_{MAX}]$, $[I_{MIN}, I_{MAX}]$ and $[\Omega_{MIN}, \Omega_{MAX}]$. For the purposes of this discussion, we leave the other orbital elements unconstrained. It will turn out that these elements constrain the possible values of range in simple ways without our having any recourse to angle rate information. Then, to the extent that we can restrict the generation of hypothetical orbits to a specified partition of the space of orbital elements, we have parallelized the task of building a catalog of objects detected within that partition. The reason is that any partition of the space of orbital elements, including the whole space itself, can be sub-divided into smaller partitions, and each sub-partition can be handled independently. In the approach outlined here, all the observations would have to be considered for each sub-partition of the space of orbit elements. However, by constructing upper and lower bounds on range for each sub-partition of the element space, we limit the number of range hypotheses that have to be considered for each sub-partition. This approach allows us to consider a manageable number of range hypotheses for each sub-partition before we generate candidate orbits, simply by making the sub-partitions small enough, so that the overall computation is feasible.
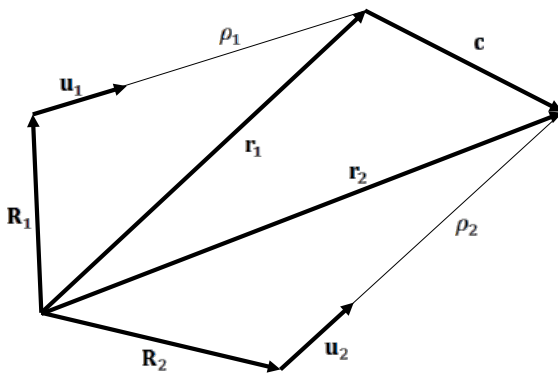
2. RANGE BOUNDARY FORMULATION

Figure 1: Vector Triangles

Assume that we have a pair of line-of-sight unit vectors $\mathbf{u}_1$ and $\mathbf{u}_2$, measured at time t_1 at station position $\mathbf{R}_1$ and time t_2 at station position $\mathbf{R}_2$, respectively. Assume, without loss of generality, that $t_2 > t_1$. We want to form the hypothesis that these two observations are associated with the same space object. To this end, we attach a set of hypothetical range values, $\{\rho_{1,m}, m = 1,2, \dots\}$ and $\{\rho_{2,n}, n = 1,2, \dots\}$ respectively, to each of these measured unit vectors and then generate candidate orbits by solving Lambert's problem for each of the pair-wise combinations of hypothetical orbital position vectors $\mathbf{r}_{1,m}$ and $\mathbf{r}_{2,n}$.

We are seeking explicit bounds on range that can be applied for each individual angle-based observation, or at most to pairs of angle-based observations. Even with the further restriction that hypothetical orbits be elliptical and Keplerian (which we accept), it may not be obvious that efficient bounds having these properties can be obtained. Exact bounds would have to be based on some admissible-region analysis of the

type developed by Milani, Tommei, Scheeres, Maruskin, Fujimoto and others. For example, denoting the gravitational parameter by μ, we write the first integrals of Keplerian motion as

$$\text{energy:} \quad E = (\dot{\mathbf{r}} \cdot \dot{\mathbf{r}})/2 - \mu/\|\mathbf{r}\| = -\mu/2a \tag{i}$$
$$\text{angular momentum:} \quad \mathbf{h} = \mathbf{r} \times \dot{\mathbf{r}} \tag{ii}$$
$$\text{Laplace vector:} \quad \mu\mathbf{e} = \dot{\mathbf{r}} \times (\mathbf{r} \times \dot{\mathbf{r}}) - \mu\mathbf{r}/\|\mathbf{r}\| \tag{iii}$$

These can be evaluated with the vector triangle relation $\mathbf{r} = \mathbf{R} + \rho\mathbf{u}$ and its time derivative $\dot{\mathbf{r}} = \dot{\mathbf{R}} + \dot{\rho}\mathbf{u} + \rho\dot{\mathbf{u}}$ for each observation. Then, for each observation, we can define admissible regions in the $(\rho, \dot{\rho})$ plane for each partition in the space of elements by means of inequalities such as

$$-\mu/(2a_{\text{MIN}}) \leq E \leq -\mu/(2a_{\text{MAX}}) \tag{iv}$$
$$\cos I_{\text{MAX}} \leq (\mathbf{h}/\|\mathbf{h}\|) \cdot \mathbf{k} \leq \cos I_{\text{MIN}} \tag{v}$$
$$e_{\text{MIN}} \leq \|\mathbf{e}\| \leq e_{\text{MAX}} \tag{vi}$$

Here $\mathbf{k}$ is the north polar unit vector in the Earth-centered inertial frame. For each observation, the values of range and range rate that satisfy these inequalities will result in orbits that lie only within the given partition of the space of elements. DeMars and Jah [6] have shown what the admissible regions look like for partitions of semimajor axis and eccentricity by a numerical treatment of the above inequalities. Maruskin, *et al.*, [7] have shown how the admissible regions evolve in time and how the overlap of the admissible regions for different observations can help solve the data association problem. However, even though expressions (i) through (vi) can be reduced to polynomial forms in range and range rate, each relation is coupled in both variables and the polynomial degree is high, preventing us from obtaining explicit expressions for range and range rate in terms of the given data. Moreover, the usual admissible-region analysis leads nowhere if angle rates are not available. For example, the track-initiation method of DeMars, *et al.*, [8], involving multiple hypotheses on range and range rate, requires both angle and angle rate values.

In the present analysis, we take a geometric and kinematic approach that does lead to explicit upper and lower bounds on the possible values of range for each observation or pair of observations, given only angle data at discrete times. In fact, we find several inequalities that must be satisfied simultaneously, and we can take the most restrictive superposition of the different bounds as our working result. In case angle rates are available, we can obtain explicit upper and lower bounds on range rate, as well as additional bounds on range. It may happen that, for a given observation, there are no values of the range or range rate that lead to orbits within the given element-space partition, so that the observation can be eliminated from further consideration. We obtain explicit conditions for the existence of possible values of range and range rate, in terms of the observation itself.

The price for obtaining explicit bounds on range and range rate is that the bounds are not exact but somewhat conservative. Although every orbit within the element-space partition corresponds to values of range and range rate that lie within the bounds given here, some values of range or range rate that satisfy the bounds may lead to orbits that lie outside the given partition. This situation represents inefficiency in the parallelization of building the catalog: nearly the same candidate orbits near the boundaries of the element-space partitions may be generated in both of the adjacent partitions, if the range or range rate hypotheses are planted densely enough. On the other hand, no candidate orbits within the given element-space partitions will be missed because of the bounds given here. The extent and cost of the inefficient duplication of candidate orbits will depend on the particular datasets and element partitions of interest, and may require further study. In practice, of course, within any element partition, any of these extra orbit hypotheses can be either kept or discarded. If they are kept, one would have, at most, a bookkeeping problem of transferring the extra orbits to the correct element partition. The trade-off in this case is that merely moving data between processors always takes time.

First, we present bounds on range that must hold for each observed line of sight. Assuming that all orbits of interest are elliptical, require that the orbital radii lie between the maximum specified apogee and the minimum specified perigee:

$$a_{\text{MIN}} (1 - e_{\text{MAX}}) \leq \|\mathbf{r}\| \leq a_{\text{MAX}}(1 + e_{\text{MAX}}) \tag{1}$$

The values of range that correspond to these limits on orbital radius can be found explicitly using the vector triangle relationship $\mathbf{r} = \mathbf{R} + \rho\mathbf{u}$. Squaring terms to remove the radical, we have

$$a_{\text{MIN}}^2(1 - e_{\text{MAX}})^2 \leq \mathbf{R} \cdot \mathbf{R} + 2(\mathbf{R} \cdot \mathbf{u})\rho + \rho^2 \leq a_{\text{MAX}}^2(1 + e_{\text{MAX}})^2 \tag{2}$$

Consider the perigee and apogee cases separately. For the perigee case, we require the orbital radius to be no smaller than the smallest allowable perigee radius:

$$\rho^2 + 2(\mathbf{R} \cdot \mathbf{u})\rho - [a_{\text{MIN}}^2(1 - e_{\text{MAX}})^2 - \mathbf{R} \cdot \mathbf{R}] \geq 0 \tag{3}$$

We will have real roots if and only if the argument of the square root of the solution is non-negative:

$$a_{\text{MIN}}^2(1 - e_{\text{MAX}})^2 \geq \mathbf{R} \cdot [\mathbf{R} - (\mathbf{R} \cdot \mathbf{u})\mathbf{u}] \tag{4}$$

If no real roots of the quadratic expression (3) exist, then we can immediately discard the current observation and form no hypotheses with it. The reason is that no value of the range will be found for this observation, which is consistent with the specified intervals of the orbital elements.

Descartes' rule of signs tells us the number of positive real roots. If the third coefficient in the quadratic form (3) is negative, that is, if $a_{\text{MIN}}^2(1 - e_{\text{MAX}})^2 > \mathbf{R} \cdot \mathbf{R}$, then, regardless of the sign of the second coefficient $2(\mathbf{R} \cdot \mathbf{u})$, we will have one positive real root and necessarily also one negative root. Because the quadratic is concave-up, the inequality is satisfied to the left of the negative root and to the right of the positive root. We can ignore the negative root and all values to the left of it, because we require *a priori* that range values to be non-negative. What remains is a positive lower limit on the possible values of range:

$$\rho \geq -(\mathbf{R} \cdot \mathbf{u}) + \sqrt{(\mathbf{R} \cdot \mathbf{u})^2 + [a_{\text{MIN}}^2(1 - e_{\text{MAX}})^2 - \mathbf{R} \cdot \mathbf{R}]} \tag{5}$$

It is worth noting that, for Earth-bound stations, the third coefficient of (3) will essentially always be negative because the inequality $a_{\text{MIN}}^2(1 - e_{\text{MAX}})^2 > \mathbf{R} \cdot \mathbf{R}$ is approximately the condition that the minimum allowable perigee radius be larger than the Earth radius. Moreover, the second coefficient $2(\mathbf{R} \cdot \mathbf{u})$ will essentially always be positive because observations have to be taken above the local horizontal plane at some positive local elevation angle.

For space-based observing stations, it is possible that neither of these circumstances would be true: the station's orbital position may be higher than the minimum specified perigee radius, or observations may be taken at negative local elevation angles, or both. If the third coefficient in (3) is positive, that is, if $a_{\text{MIN}}^2(1 - e_{\text{MAX}})^2 < \mathbf{R} \cdot \mathbf{R}$, then the quadratic will have either no positive real roots or two positive real roots, depending on the sign of the second coefficient. If, furthermore, the second coefficient in (3) is positive, that is, if $(\mathbf{R} \cdot \mathbf{u}) > 0$, then we have no positive real roots, but only a pair of negative roots. Because the quadratic is concave-up, the inequality (3) is satisfied to the left of the more negative root and to the right of the less negative root. However, since we require *a priori* that range values be non-negative, we are left merely with the condition that $\rho \geq 0$. If the second coefficient is negative, that is, $(\mathbf{R} \cdot \mathbf{u}) < 0$, meaning that the observation is taken at negative local elevation angle, then the quadratic will have two positive real roots. Because the quadratic is concave-up, the inequality (3) will be satisfied to the left of the smaller root, that is, between $\rho = 0$ and the smaller root, and also to the right of the larger root. In this case, we have two disjoint intervals of range, one finite and one semi-infinite, over which range hypotheses will satisfy the perigee constraint:

$$0 \leq \rho \leq -(\mathbf{R} \cdot \mathbf{u}) - \sqrt{(\mathbf{R} \cdot \mathbf{u})^2 + [a_{\text{MIN}}^2(1 - e_{\text{MAX}})^2 - \mathbf{R} \cdot \mathbf{R}]} \tag{6}$$

$$\rho \geq -(\mathbf{R} \cdot \mathbf{u}) + \sqrt{(\mathbf{R} \cdot \mathbf{u})^2 + [a_{\text{MIN}}^2(1 - e_{\text{MAX}})^2 - \mathbf{R} \cdot \mathbf{R}]} \tag{7}$$

Now we consider the apogee case and seek to derive results that are analogous to those above. The apogee case will provide us with conditions on values of the range that are complementary to those of the perigee case. Since both sets of conditions must be satisfied simultaneously, we can take the most restrictive superposition of all conditions on range to define the set of values over which we must form range hypotheses.

For the apogee case, we have from the inequality (2) that the orbital radius must be no larger than the maximum allowable apogee radius:

$$\rho^2 + 2(\mathbf{R} \cdot \mathbf{u})\rho - [a_{MAX}^2(1 + e_{MAX})^2 - \mathbf{R} \cdot \mathbf{R}] \leq 0 \tag{8}$$

We will have real roots if and only if the argument of the square root in the solution is non-negative:

$$a_{MAX}^2(1 + e_{MAX})^2 \geq \mathbf{R} \cdot [\mathbf{R} - (\mathbf{R} \cdot \mathbf{u})\mathbf{u}] \tag{9}$$

If no real roots exist, then we can immediately discard the observation and form no hypotheses with it. The reason is that no value of the range will be found for this observation, which is also consistent with the specified intervals of the orbital elements. Assuming that we have real roots in equation (8), we use Descartes' rule of signs to determine the number of positive real roots. If the third coefficient in the quadratic form (8) is negative, that is, if $a_{MAX}^2(1 + e_{MAX})^2 > \mathbf{R} \cdot \mathbf{R}$, then, regardless of the sign of the second coefficient $2(\mathbf{R} \cdot \mathbf{u})$, we will have one positive real root and necessarily also one negative root. Because the quadratic is concave-up, the inequality (8) is satisfied between the roots. Moreover, we require *a priori* that range values be non-negative, so we can say without loss of generality that the inequality will be satisfied between $\rho = 0$ and the positive real root. The result is that we have an upper bound on the possible values of range:

$$0 \leq \rho \leq -(\mathbf{R} \cdot \mathbf{u}) + \sqrt{(\mathbf{R} \cdot \mathbf{u})^2 + [a_{MAX}^2(1 + e_{MAX})^2 - \mathbf{R} \cdot \mathbf{R}]} \tag{10}$$

As before, for Earth-bound stations, the third coefficient will essentially always be negative because the inequality $a_{MAX}^2(1 + e_{MAX})^2 > \mathbf{R} \cdot \mathbf{R}$ is approximately the condition that the maximum allowable apogee radius be larger than the Earth radius. Moreover, the second coefficient $2(\mathbf{R} \cdot \mathbf{u})$ will essentially always be positive because observations have to be taken above the local horizontal plane at some positive local elevation angle.

Also as before, for space-based observing stations, it is possible that neither of these circumstances would be true: the station's orbital position may be above the maximum specified apogee radius, or observations may be taken at negative local elevation angles, or both. If the third coefficient in (8) is positive, that is, if $a_{MAX}^2(1 + e_{MAX})^2 < \mathbf{R} \cdot \mathbf{R}$, then the quadratic will have either no positive real roots or two positive real roots, depending on the sign of the second coefficient. This is the possibility just mentioned for space-based stations, although we do not expect this case for Earth-bound stations. If, furthermore, the second coefficient in (8) is positive, that is, if $(\mathbf{R} \cdot \mathbf{u}) > 0$, then we have no positive real roots, but only a pair of negative roots. Because the quadratic is concave-up, the inequality (8) is satisfied between these roots. However, since we require *a priori* that range values be non-negative, we can discard this particular observation and form no range hypotheses for it.

If the third coefficient in (8) is positive, but the second coefficient is negative, $(\mathbf{R} \cdot \mathbf{u}) < 0$, meaning that the observation is taken at negative local elevation angle, then the quadratic will have two positive real roots. The quadratic is concave-up, so the inequality (8) will be satisfied between these two roots. In this case, we have a single finite interval of range over which range hypotheses will satisfy the apogee condition:

$$\rho \geq -(\mathbf{R} \cdot \mathbf{u}) - \sqrt{(\mathbf{R} \cdot \mathbf{u})^2 + [a_{MAX}^2(1 + e_{MAX})^2 - \mathbf{R} \cdot \mathbf{R}]} \tag{11}$$

$$\rho \leq -(\mathbf{R} \cdot \mathbf{u}) + \sqrt{(\mathbf{R} \cdot \mathbf{u})^2 + [a_{MAX}^2(1 + e_{MAX})^2 - \mathbf{R} \cdot \mathbf{R}]} \tag{12}$$

The set of range values over which we may have to form hypotheses for the observation in question is given by the intersection of all of the above conditions, both perigee conditions and apogee conditions.

The above conditions are bounds on the possible values of range, which can be computed for each single observation. The fact that only single observations are involved is what allows us to find explicit bounds for each of the ranges before we form any range hypotheses. However, at least five additional restrictions on the allowable

values of range can be deduced from relations that involve both of the ranges presented for a solution to Lambert's problem. Although the nonlinearities in these relations prevent us from getting explicit inequalities like (5) – (7) and (10) – (12), nevertheless we can formulate additional conditions that ρ_1 and ρ_2 must satisfy. Checking these extra conditions for each range pair may keep us from having to produce some unnecessary and relatively expensive Lambert solutions.

Using the vector triangle relation for each of the two lines of sight, compute the unit vector $\mathbf{n}$ normal to the candidate orbital plane:

$$\mathbf{n} = \pm\,(\mathbf{r}_1 \times \mathbf{r}_2)/\|\mathbf{r}_1 \times \mathbf{r}_2\| \tag{13}$$

Here the ambiguous sign is resolved as "+" for "short-way" trajectories and "–" for "long-way" trajectories. The inclination is given unambiguously by

$$\cos I = \mathbf{n} \cdot \mathbf{k} \tag{14}$$

The inclination of the candidate orbit lies in the specified interval $[I_{\text{MIN}}, I_{\text{MAX}}]$ provided that $\cos I$ lies in the interval $[\cos I_{\text{MAX}}, \cos I_{\text{MIN}}]$. Hence we require that

$$\cos I_{\text{MAX}} \leq \mathbf{n} \cdot \mathbf{k} \leq \cos I_{\text{MIN}} \tag{15}$$

In a similar way, we use the unit nodal vector to obtain conditions that the range pair must satisfy if the candidate orbit is to lie within a specified interval of right ascension of the ascending node, $[\Omega_{\text{MIN}}, \Omega_{\text{MAX}}]$. In the Earth-centered inertial frame, we have

$$(\mathbf{k} \times \mathbf{n})/\|\mathbf{k} \times \mathbf{n}\| = (\cos\Omega, \sin\Omega, 0)^{\text{T}} \tag{16}$$

so that, following standard logic for quadrant resolution, we require

$$\Omega_{\text{MIN}} \leq \tan^{-1}(\sin\Omega/\cos\Omega) \leq \Omega_{\text{MAX}} \tag{17}$$

Of course, for important special cases like near-GEO orbits, it may be preferable to define element-space partitions in terms of nonsingular elements such as $p \triangleq \sin(I/2)\cos\Omega$ and $q \triangleq \sin(I/2)\sin\Omega$. No special difficulty attaches to working in terms of these or any other elements related to the orbit plane. If any range-pair hypothesis (ρ_1, ρ_2) does not satisfy all of the above conditions, then that pair of values can be eliminated from further consideration without solving Lambert's problem. Note that it is the pair of range values that is eliminated; either range value by itself may still lead to an acceptable hypothesis in combination with some other range value.

Next, we can use three special solutions of Lambert's problem to restrict the ranges. The eccentricity of the orbit of least possible eccentricity that goes through a given pair of position vectors can be computed solely in terms of those position vectors. Call it e_0. Likewise, the semimajor axis of the orbit of least possible semimajor axis that goes through the pair of positions can be computed solely in terms of the position vectors. Call it a_0. Hence, for each hypothesized range pair (ρ_1, ρ_2), we compute the corresponding position vectors and apply the following logic:

> If $a_0 > a_{\text{MAX}}$, then reject the hypothesis pair without solving Lambert's problem, because the geometry is guaranteed to produce a larger semimajor axis than we have specified.

> If $e_0 > e_{\text{MAX}}$, then reject the hypothesis pair without solving Lambert's problem, because the geometry is guaranteed to produce a larger eccentricity than we have specified.

Of course, even for a (ρ_1, ρ_2) hypothesis that passes the above tests, the actual solution of Lambert's problem may still turn out to get rejected once we have computed the elements of the candidate orbit. The reason is that none of the conditions on range derived above involves the minimum allowable eccentricity, e_{MIN}. This fundamental feature of our problem raises the question of how well we can limit the generation of candidate orbits to lie within the given eccentricity interval. Let us assume that the hypothetical range pair is not rejected by the above criterion, so that $e_0 \leq e_{\text{MAX}}$. Assume also that all of the range bounds and other conditions that depend on single observations have already been applied. Then we know that the Lambert solution for a pair of range hypotheses will not produce an orbit having eccentricity outside the interval $[e_0, e_{\text{MAX}}]$. If $e_{\text{MIN}} \leq e_0$, we have no difficulty: the candidate orbit

will have an eccentricity within the given interval $[e_{MIN}, e_{MAX}]$. However, if $e_0 < e_{MIN}$, then the eccentricity of the candidate orbit may or may not lie within the specified interval. The Lambert solution has to be generated and then either kept if the eccentricity is at least as large as e_{MIN} or discarded if the candidate eccentricity turns out to be less than e_{MIN}. This represents some inefficiency in the generation of candidate orbits, especially if those same candidate orbits were to be generated in the processing for other element-space partitions. The extent of the overall inefficiency depends on the dataset and the actual element-space partitions being used, so we cannot draw general conclusions. It would be helpful at this point to have reasonably sharp bounds on the actual eccentricity in the Lambert problem without having to solve the whole problem. However, lacking that, we have no better recourse than to generate the candidate orbit. Overall, we do expect to be able to reduce the number of Lambert solutions that have to be generated, compared to the number required without the above checks involving a_0 and e_0.

The formulas for a_0 and e_0 are well known:

$$4a_0 = \|\mathbf{r}_1\| + \|\mathbf{r}_2\| + \|\mathbf{r}_2 - \mathbf{r}_1\| \quad \text{and} \quad e_0 = \frac{|(\|\mathbf{r}_1\| - \|\mathbf{r}_2\|)|}{\|\mathbf{r}_2 - \mathbf{r}_1\|} \tag{18}$$

Finally, Euler's Theorem, a special case of Lambert's Theorem, expresses the time of flight Δt_P between given position vectors on a parabolic (zero-energy) orbit:

$$\Delta t_P = \frac{4}{3}\sqrt{\frac{a_0^3}{\mu}}(1 - s\,\lambda^3) \tag{19}$$

Here the quantity s is a signum function: $s = +1$ for "short-way" trajectories and $s = -1$ for "long-way" trajectories. The parameter λ is defined in terms of the position vectors:

$$0 \leq \lambda^2 = \frac{\|\mathbf{r}_1\| + \|\mathbf{r}_2\| - \|\mathbf{r}_2 - \mathbf{r}_1\|}{\|\mathbf{r}_1\| + \|\mathbf{r}_2\| + \|\mathbf{r}_2 - \mathbf{r}_1\|} \leq 1 \tag{20}$$

Because, for given position vectors, the time of flight in Lambert's problem is a monotonic decreasing function of the orbital energy, elliptic (negative-energy) orbits will always have a time of flight longer than the parabolic time, and hyperbolic (positive-energy) orbits will always have a time of flight shorter than the parabolic time. In our case, we can require that our observation pairs and range hypotheses always produce elliptic orbits:

$$t_2 - t_1 > \Delta t_P \tag{21}$$

Combinations that do not satisfy this condition can be eliminated without generating a Lambert solution. Given an observation pair $\mathbf{u}_1$ and $\mathbf{u}_2$, the previous formulas, and the associated logic, can be used to decide if a hypothetical pair of ranges should be used to generate a Lambert solution. Of course, whatever Lambert solutions are generated should be verified for compliance with the specified interval of eccentricity, because none of the conditions on range derived so far depends on the value of the minimum allowable eccentricity e_{MIN}. By construction, we have guaranteed compliance with the intervals of semimajor axis, inclination and right ascension of the ascending node.
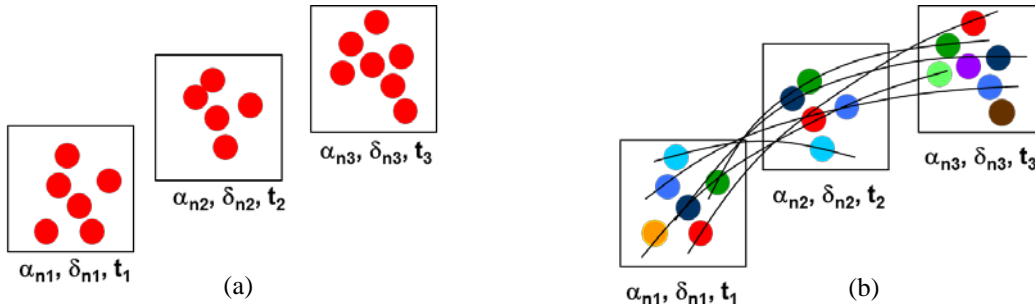

Figure 2: (a) Raw unidentified observations (b) Observations that have been randomly connected together

3. APPLYING RANGE BOUNDARIES TO RANGE ESTIMATION

Now that we have defined a set of rigorous boundaries for candidate range estimates, we can combine these boundaries with traditional range estimation procedures for angles-only IOD. First, blindly generate all possible combinations of observations (see Figure 2). Next, using the method of Gauss, estimate ranges for each of the observations within a given combination using the techniques outlined in [5] and [9]. It is not necessary to finish the IOD process. At this stage we only calculate the range estimates for each observation in a draw. Filter these range estimates for obviously invalid solutions before applying the orbit element boundaries to further eliminate infeasible solutions. The last step is to check range estimates for consistency and persistence across combinations returning potentially valid solutions.

	Obs. Indices	ρ_1	ρ_2	ρ_3	
1	(1,10,19)	412	457	435	PASS
2	(1,10,28)	420	475	490	PASS
3	(1,17,28)	364	621	400	FAIL
	…	…	…	…	
m	(2,11,29)	537	545	523	PASS
m+1	(2,21,35)	678	323	721	FAIL

Table 2: Estimates of range for various random draws of observations.

Here we introduce the concept of *consistency* and *persistence*. These concepts hinge upon the notion that all IOD range estimates will be inaccurate and unrefined but generated using a common method. Using consistency and persistence, we will assign the random draws of observations into one of three categories: *Not Likely*, *Likely*, and *More Likely*. Obviously, failed cases automatically go into the *Not Likely* category.

Observation ID Numbers							
1	10	19	28				
2	11	18	20	29			
3	12	19	21	30	32		
4	13	21	22	31	33		
5	14	23	32				
6	15	24	33				
7	16	25	34				
8	17	26	35				
9	18	27	36				
10	1	19	28				
11	2	20	27	29	32		
12	3	21	30				
13	4	22	31				
14	5	23	32				
15	6	24	33				
16	7	25	34				
17	8	19	26	32	35		
18	2	9	22	27	36		
19	1	3	10	17	28	32	
20	2	11	29				
21	3	4	12	30	33		
22	2	4	13	18	31		
23	5	14	32				
24	6	15	33				
25	7	16	34				
26	8	17	35				
27	9	11	18	32	36		
28	1	10	19				
29	2	11	20				
30	3	12	21				
31	4	13	22				
32	3	5	11	14	17	19	23	27
33	4	6	15	21	24		
34	7	16	25				
35	8	17	26				
36	9	18	27				

Table 1: Persistence table where all valid associations between individual observations can be seen.

There are two types of consistency. The first is consistency of range estimates within a random draw. For cases where the normalized time between observations is small, then physics dictates that the range estimates across the three observations would be roughly similar. The second is consistency of range estimates for a specific observation across all random draws. Many bad cases will be caught by the orbit element boundaries but one can also establish a mean and variance for the estimate of range associated with each observation. These two types of consistency can be used to distinguish outlier range estimates if there is trouble discerning which of several valid random draws should be flagged as more or less likely.

Consistent solutions can coalesce into persistent solutions. A persistent solution occurs when a particular observation is repeatedly associated with another observation in the list of valid random draws. Table 1 shows a list of hypothetical range estimates for different sets of observation combinations. Individual cases are first screened for validity based upon the orbit element boundaries described previously and are marked pass or fail. Consider the

Ranking	Obs
More Likely	(1,10,19,28)
More Likely	(2,11,20,29)
More Likely	(3,12,21,30)
…	…
Likely	(1,10,19)
Likely	(2,11,20)
…	…
Not Likely	(1,10,33)
Not Likely	(2,21,35)
Not Likely	(5,17,24)

Table 3: Ranking of the persistent and consistent solutions.

observation triplets (1,10,19) and (10,19,28) that have both passed the orbit element boundary tests meaning that these are *Likely* observation pairings. We can check the range estimates for observation 10 and 19 for consistency if desired to further distinguish observation groupings. However, persistence says that if (1,10,19) as well as (10,19,28) are likely valid, then (1,10,19,28) must also be a *Likely* grouping of observations.

Following this process for all valid observation draws, we can generate Table 2 where our initial valid groupings of three observations have been strung together into groups of four or more observations. Looking at row one, we see that observation 1 associated only with 10, 19, and 28. Furthermore, row 10 indicates that observation 10 associated only with 1, 19, 28. Likewise, row 28 indicates that observation 28 associated only with 1, 10, and 19. However, observation 19 on row 19 associated with 1, 3, 10, 17, 28, 32. Using persistence, we can say that the association between 1, 10, 19, and 28 is *More Likely* because 3 out of the 4 observations associated only with each other and the fourth observation associated with a few additional observations. The question then is should we toss out the candidate grouping of (19, 1, 3, 10, 17, 28, 32)? To be conservative one can flag this case as *Likely* and maintain it in a multiple hypothesis setting. One could also look at the consistency checks for each range estimate to make a further discrimination of likelihood. However, further inspection of Table 2 reveals that observations 3, 17, and 32 are more strongly associated with other observations. Therefore, one could safely demote this candidate grouping in the rankings.

Proceeding through each row of Table 2, we generate a ranking of hypothetical observation groupings in Table 3. Cases where certain groupings of observations associated only with themselves are flagged as *More Likely*. The one-off cases of extended groupings can be maintained as *Likely* or demoted in the rankings. In any case, one should always maintain the original set of valid three-observation groupings as *Likely* in addition to the built-up groupings. All of the final ranked observation groupings can now be used to generate candidate orbits in a multiple hypothesis sense to examine refined orbit solutions. Essentially this use of persistence and consistency allows us to perform a "poor man's version" of the classical assignment problem. Future work will attempt to employ the formal methodologies of the classical assignment problem with the range estimate consistency checks as a cost function. Our hope would be to determine a more nearly optimal set of observation assignments.

4. A MONTE CARLO SIMULATION

Using a simple two-body orbit propagator, angles-only observations of Intelsat-8 were simulated as viewed from PanSTARRS on top of Mt. Haleakala (203.74° longitude, 20.71° latitude, 3.07 km elevation about the WGS-95 geoid). Observations were obtained two hours apart over a 24 hour period for a total of 13 observations. One observation was selectively "bumped" with a random Gaussian N(120,120) arc-second error. Using the above outlined approached, each of the 13 observations was thrown into a "bucket" and drawn blindly in groupings of 4 observations at a time leading to a possible 715 combinations. Of these 715 combinations, 220 combinations contained the "bumped" or "bad" observation. The question to be answered is "Can we prune out the hypotheses with the bad observation *a priori*?" Using the range estimation procedure detailed above, the range estimates were computed for each of the 715 combinations of 4 observations. The physics-based boundaries were tailored for a GEO object and set at semi-major axis in the interval [37500, 45000] km, eccentricity in [0, 0.075], and inclination in [-12°, 12°]. The range estimates could fail for a variety of reasons including poor geometry and negative range estimates. Only hypotheses that returned a valid solution were subjected to the orbit element boundary filters. This process was repeated in a Monte Carlo fashion for 1000 trials with a specified observation having random error applied to it. The results of this simulation were that out of the 715,000 total hypotheses over 1000 trials, only 2968 cases passed through the various validation procedures and resulted in a false association. This means that we had a 0.42% acceptance rate for the bad observation.

5. A GEO CLUSTER SIMULATION

Now we consider the case of a GEO cluster of 9 satellites separated by 0.25° in right ascension of the ascending node. For each of the nine objects, four simulated observations 2 hours apart were generated with 2 arc seconds of error applied. In total there were 36 observations that were drawn blindly 3 at a time for a total of 7140 possible combinations. The question now is "Can we rank hypotheses in order of most likely to least likely *a priori*?" The result of this simulation is that, after computing the range estimates and applying the physics based boundaries on orbit elements, the algorithm returned valid range estimates for all of the cases that we knew to be correct plus a handful of cases that were incorrect. Using consistency and persistence to string together observations into longer arcs of data, the algorithm correctly built up the 3-observation groupings into the correct 4-observation groupings and only these cases were marked as highly likely. None of the incorrect 3-observation pairings from the previous step were included in the longer arcs of data and these were all flagged as less likely due to their unique occurrences.

6. CONCLUSION

Our results show that the possible values of both range and range rate can be limited *a priori* for each line-of-sight observation to finite intervals corresponding to a specified partition of the element space. The endpoints of the intervals are given explicitly in terms of the angle-based observations, station position and station velocity, and can be computed independently for each observation. Additional conditions based on the orientation of the orbital plane and special solutions of Lambert's problem, which must be satisfied by range values for pairs of observations, can be used to further reduce the number of Lambert solutions needed for the initial orbit determinations. All the formulas derived here apply uniformly to Earth-bound and space-based observing stations. We also present explicit conditions identifying when a given observation does not correspond to any possible orbit within the specified element-space partition. Such observations can be discarded before any data association hypotheses or Lambert solutions are produced. We have demonstrated the effectiveness of these techniques through a single satellite Monte Carlo simulation and a GEO cluster simulation. We have found that it is possible to rank observation hypotheses in rough order of likelihood *a priori*. We have found this method is also effective for culling out bad observations.

7. REFERENCES

[1] K. Muinonen and E. Bowell, "Asteroid Orbit Determination Using Bayesian Probabilities," *Icarus,* vol. 104, no. 2, pp. 255-279, 1993.

[2] J. Virtanen, K. Muinonen and E. Bowell, "Statistical Ranging of Asteroids," *Icarus,* vol. 154, no. 2, pp. 412-431, 2001.

[3] K. Fujimoto and D. J. Scheeres, "Correlation and Initial Orbit determination for Short-Arc Optical Observations," in *Proceedings of the Advanced Maui Optical and Space Surveillance Technologies Conference*, 2010.

[4] R. H. Gooding, "On the Solution of Lambert's Orbital Boundary-Value Problem," Royal Aerospace Establishment Technical Report 88027, 1988.

[5] R. Karimi and D. Mortari, "Initial Orbit Determination Using Multiple Observations," *Celestial Mechanics and Dynamical Astronomy,* vol. 109, no. 2, pp. 167-180, 2011.

[6] K. J. DeMars and M. K. Jah, "Initial Orbit Determination via Gaussian Mixture Approximation of the Admissible Region," in *Proceedings of the 22nd AAS/AIAA Space Flight Mechanics Conference*, Charleston, S.C., Feb 2, 2012.

[7] J. M. Maruskin, D. Scheeres and K. Alfriend, "Correlation of Optical Observation of Objects in Earth Orbit," *Journal of Guidance, Control, and Dynamics,* vol. 32, no. 1, pp. 194-209, Jan-Feb 2009.

[8] K. J. DeMars, M. K. Jah and P. Schumacher, "The Use of Angle and Angle Rate Data for Deep-Space Orbit Determination and Track Association," *Advances in the Astronautical Sciences,* vol. 136, 2010.

[9] H. Curtis, Orbital Mechanics For Engineering Students, Amsterdam/Boston: Elsevier Butterworth-Heinemann, 2005.